Supplement of Geosci. Model Dev., 17, 4355–4382, 2024
https://doi.org/10.5194/gmd-17-4355-2024-supplement

Geoscientific Model Development
Open Access

Supplement of

VISIR-2: ship weather routing in Python

Gianandrea Mannarini et al.

Correspondence to: Gianandrea Mannarini (gianandrea.mannarini@cmcc.it)

Table of Contents

Introduction

This supporting information provides an assessment of the impact of the interpolation schemes (S0), data on the computational performance of the VISIR-2 software (section S1), additional details about the identification of the vessel's performance (S2), two specific routes from both the ferry and the sailboat case studies (S3), all the bundles of 2022's optimal routes (S4), route duration metrics for direction-resolved sailboat routes (S5), and the computation of the angle of attack between vessel's heading and course (S6). Unless stated otherwise, all equation and table numbers should be understood to refer to those found in the main manuscript.

S0. Interpolation schemes

To evaluate the impact of two interpolation methods (Sint=0, representing the arithmetic average of edge head and tail field values; Sint=1, representing the field value at the edge barycenter), we generated three synthetic fields and edges with varying lengths and orientations. Subsequently, we compared the representative values of the edges (Fig. S0).

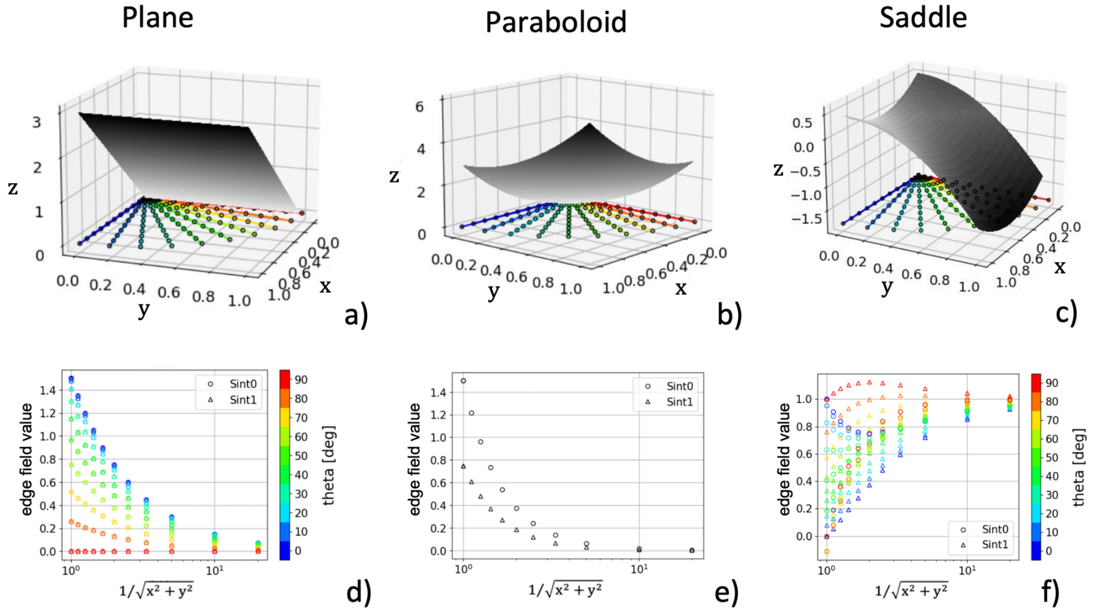

Fig. S0 a)-c) Test hypersurfaces (shaded in grey) and graph edges (coloured lines and markers indicating the edge head). d)-f) Edge representative values of the different hypersurfaces for both Sint=0 (circles) and Sint=1 (triangles).

The first field is merely a plane (Fig. S0.a), as it is a linear function of the two-dimensional coordinates. Therefore, the same outcome is anticipated for both Sint=0 and Sint=1. This expectation is verified by the results, which also demonstrate that both outcomes converge to a common value as the edge length diminishes (Fig. S0.d). Notably, directions closer to the gradient of the plane are more influenced by the edge length.
The second field is a paraboloid (Fig. S0.b). In this case, the Sint=1 scheme exhibits half the error compared to Sint=0 (Fig. S0.e). Since the field is invariant to rotation, no dependence on edge direction is observed.
The third field represents a saddle (Fig. S0.c). Larger discrepancies between Sint=0 and Sint=1 occur along the edge directions aligned with the maximum curvature of the saddle (the *y* and *x* axes). Both schemes converge to a common asymptotic value for smaller edges (Fig. S0.f).

Back to Introduction

S1. Computational performance

The assessment consisted in profiling four (Grafi, Campi, Pesi, Tracce) among the VISIR-2 modules listed in Tab.4 of the main manuscript.

Corresponding computing time T_c was recorded for numerical problems of various sizes, indexed by either the number of coast points (N_c, for just Grafi) or the number of degrees of freedom (DOF, for all other modules). The DOF was obtained as the product of the number of graph edges E and the number of time steps N_T. A submodule granularity was ensured, with profiling at the level of the main phases of processing, and the outcome is documented in Fig.S1. Data were collected via methods from both the `time` and `cProfile` python modules. The profiling times shown here were obtained on an iMac computer with 3.8 GHz 8-Core Intel Core i7 processor and 32 GB 2667 MHz DDR4 memory. Instead, the performance coefficients provided in the main manuscript were derived from performance data relative to a HPC facility as described thereto.

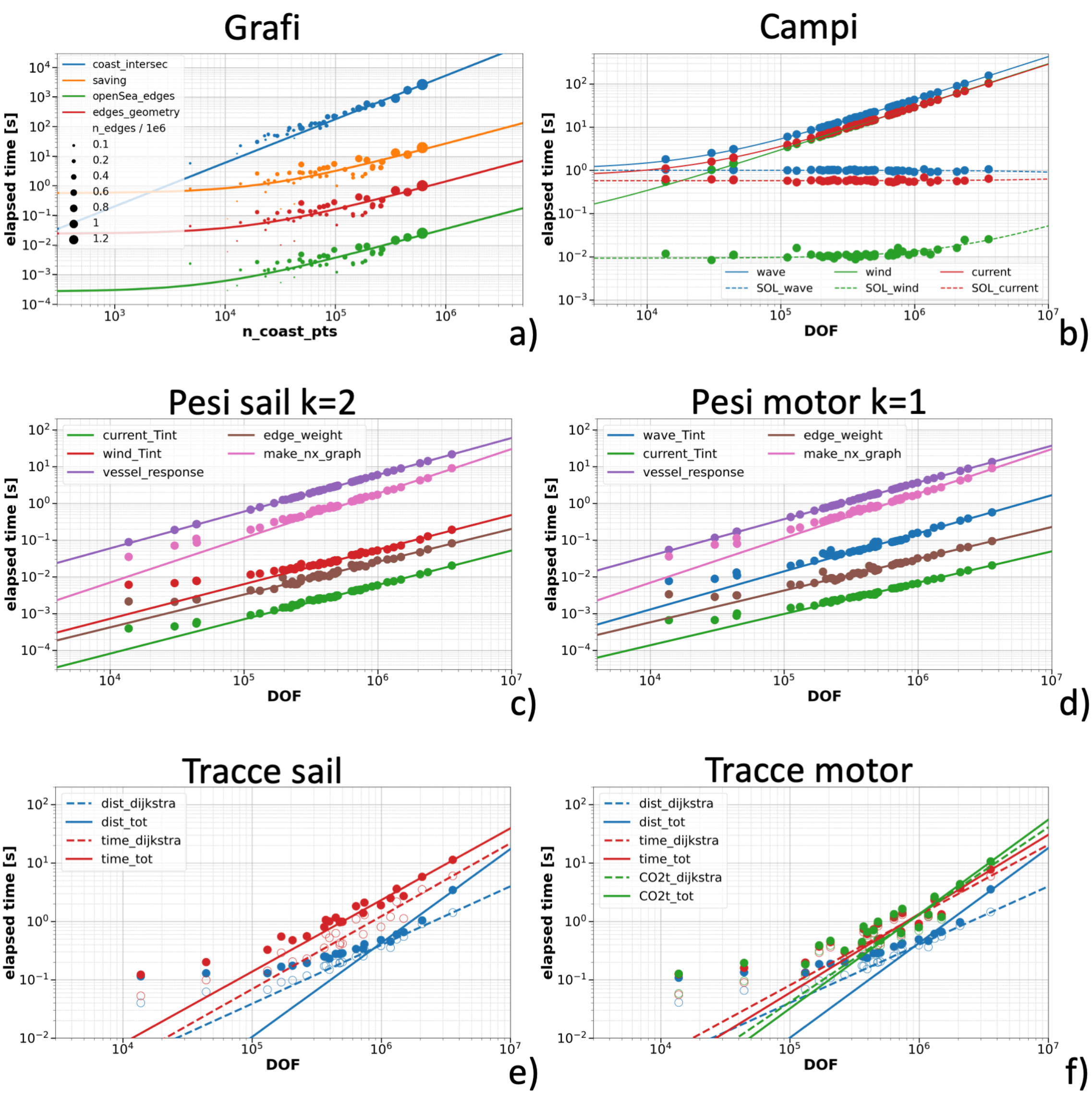

Fig. S1 Profiling of computing time for VISIR-2 main modules: a) Grafi; b) Campi; c) Pesi -sailboat version; d) Pesi - motorboat; e) Tracce- sailboat; f) Tracce - motorboat. The independent variable is the number of degrees of freedom (DOF) in the graph, but for a) where it is the number of shoreline points N_c. Markers refer to experimental data points and lines to least-square fits. In e-f) void markers refer to just the Dijkstra's component and full markers to the whole shortest path routine. The graph parameters were (ν,1/Δx)=(4,12/°). The *k* parameter in the titles of panels c) and d) refers to the number of iterations of Eq.A1. In both Campi and Pesi the Sint=1 option was used, representing a worst-case estimate of the computing time (cf. manuscript Sect.2.3.2).

submodule	description	fit fun	fit coeffs			
			a	std	b	std
coast_intersec	pruning coast-intersecting edges	y = ax ^ b	8.00E-06	3.00E-06	1.47E+00	3.41E-02
saving	node, edges, and coastline saving	y = a + bx	5.64E-01	3.37E-01	2.62E-05	2.06E-06
openSea_edges	find edges in open sea	y = a + bx	2.68E-04	3.83E-04	3.48E-08	2.34E-09
edges_geometry	edges center, orientation, and length saving	y = a + bx	2.39E-02	1.75E-02	1.38E-06	1.07E-07

Tab.S1 Fit coefficients of the T_c= *a* DOF*^{b} regressions for various components of the Grafi module. *Std* are the standard deviation errors on *a* and *b*. Based on data of Fig.S1.

submodule	description	fit fun	fit coeffs			
			a	std	b	std
wave	spatial interpolation of wave height and direction over edges	y = a + bx	1.06E+00	9.59E-02	4.32E-05	1.06E-07
SOL_wave	seaoverland application over waves fields		1.01E+00	7.04E-03	-9.63E-09	7.82E-09
wind	spatial interpolation of wind speed and direction over edges		4.94E-02	5.33E-02	2.96E-05	5.92E-08
SOL_wind	seaoverland application over wind fields		9.37E-03	3.64E-04	4.26E-09	4.04E-10
current	spatial interpolation of currents over edges		7.33E-01	3.05E-02	2.87E-05	3.38E-08
SOL_current	seaoverland application over currents fields		5.79E-01	6.65E-03	5.45E-09	7.38E-09

Tab.S2 As Tab.S1 but for the Campi module.

description	fit fun	fit coeffs							
		sail				motor			
		a	std	b	std	a	std	b	std
time interpolation of wave height and direction over timesteps	y = ax^b					9.33E-08	2.04E-08	1.04E+00	1.51E-02
time interpolation of currents over timesteps		1.29E-08	9.66E-10	9.45E-01	5.23E-03	5.43E-08	6.50E-09	8.52E-01	8.40E-03
time interpolation of wind speed and direction over timesteps		3.80E-08	9.70E-09	1.02E+00	1.77E-02				
STW evaluation		4.24E-06	3.66E-08	9.96E-01	5.99E-04	3.77E-06	8.28E-08	1.00E+00	1.52E-03
SOG and edge delay comupation		1.44E-07	3.75E-08	8.75E-01	1.83E-02	2.04E-07	3.58E-08	8.65E-01	1.23E-02
populating networkX graph		4.50E-08	1.53E-08	1.27E+00	2.32E-02	9.86E-08	2.45E-08	1.21E+00	1.70E-02

Tab.S3 As Tab.S1 but for the Pesi module. Data for the case *k*=1 in the iterative solution of the transcendental equation, Eq.A1.

submodule	description	fit fun	fit coeffs							
			sail				motor			
			a	std	b	std	a	std	b	std
wave_Tint	time interpolation of wave height and direction over timesteps	y = ax^b					5.67E-08	1.32E-08	1.07E+00	1.61E-02
current_Tint	time interpolation of currents over timesteps		1.49E-08	1.42E-09	9.35E-01	6.65E-03	1.40E-08	2.08E-09	9.41E-01	1.04E-02
wind_Tint	time interpolation of wind speed and direction over timesteps		1.26E-07	2.95E-08	9.41E-01	1.63E-02				
vessel_response	STW evaluation		5.93E-06	9.64E-08	1.00E+00	1.13E-03	5.11E-06	5.13E-08	9.98E-01	6.96E-04
edge_weight	SOG and edge delay comupation		1.15E-07	2.04E-08	8.93E-01	1.24E-02	1.92E-07	3.74E-08	8.69E-01	1.37E-02
make_nx_graph	populating networkX graph		1.02E-07	2.43E-08	1.21E+00	1.63E-02	9.25E-08	2.27E-08	1.22E+00	1.68E-02

Tab.S4 As Tab.S3, but for *k*=2.

submodule	description	fit fun	fit coeffs							
			sail				motor			
			a	std	b	std	a	std	b	std
dist_dijkstra	least distance route computation	y = ax^b	2.12E-07	8.01E-08	1.04E+00	2.59E-02	3.70E-07	1.05E-07	1.00E+00	1.96E-02
dist_tot	least distance route, track metrics and save ouput files		3.50E-08	3.40E-08	1.22E+00	6.59E-02	1.11E-07	8.77E-08	1.14E+00	5.39E-02
time_dijkstra	least time route computation		1.33E-06	5.47E-07	1.01E+00	2.82E-02	1.35E-06	4.92E-07	1.01E+00	2.52E-02
time_tot	least time route, track metrics and save ouput files		1.48E-06	7.98E-07	1.02E+00	3.70E-02	1.05E-06	5.15E-07	1.04E+00	3.37E-02
CO2t_dijkstra	least CO2 route computation						1.90E-07	9.54E-08	1.16E+00	3.43E-02
CO2t_tot	least CO2 route, track metrics and save ouput files						1.87E-07	1.10E-07	1.18E+00	4.04E-02

Tab.S5 As Tab.S1 but for the Tracce module.

[Back to Introduction](#)

S2. Vessel performance

For both vessels considered in the manuscript, the ferry and the First-367 sailboat, a function with its seakeeping performance is identified starting from a look-up table (LUT). As explained in the main manuscript, the LUT stems from either a simulator (for the ferry) or a velocity prediction programme (VPP, for the sailboat). The function used to encode the seakeeping performance can be either a cubic spline or a neural network. The predictions (evaluations at new values of the independent variable) deriving from such functions are compared to the "observations" (data from the LUT) and relative scores are presented in this section.

S2.1 Ferry

The ferry is the 125-m long vessel which principal particulars are given in Tab.2 of the main manuscript. The scores (Pearson's R^2 coefficient, root mean square error RMSE) from both the spline and neural network are given in the following two subsections. It is distinguished between the speed through water (STW) and the CO_2 emission rate.

S2.1.1 Spline

The Bspline method[1] is used, and the outcome is provided in the figure below.

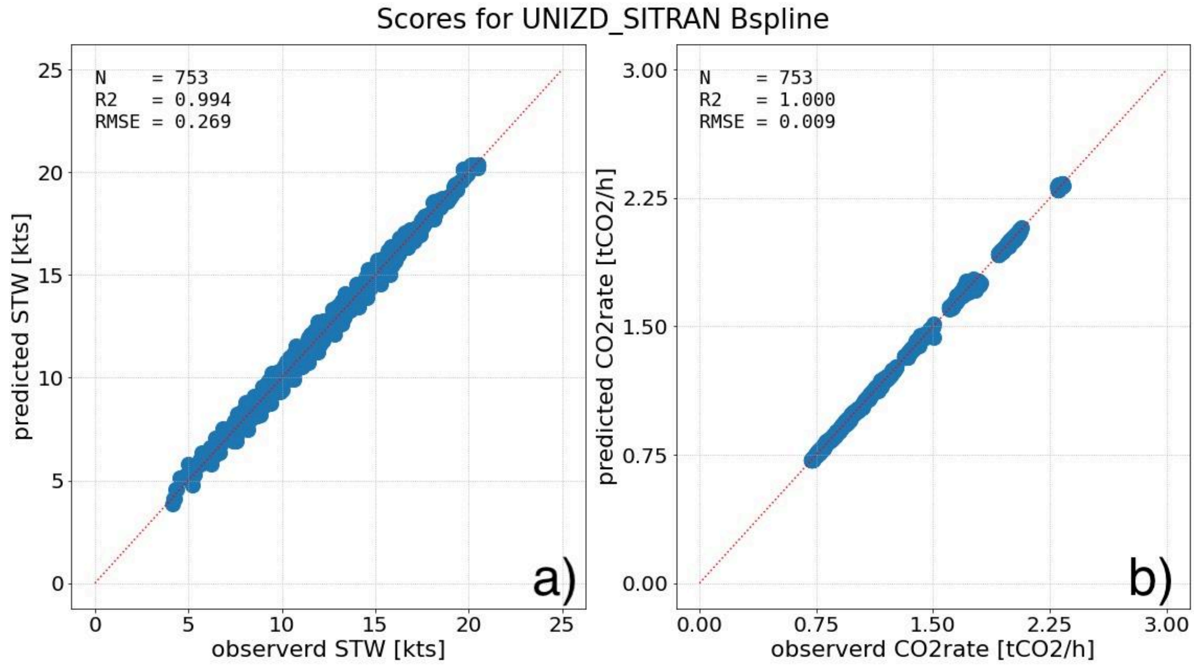

Fig.S2 Predicted vs, observed STW (a) and CO_2 emission rate (b) of the ferry, using the spline interpolation on the vessel's LUT.

[1] https://docs.scipy.org/doc/scipy/reference/generated/scipy.interpolate.BSpline.html

S2.1.2 Neural Network

The parameters of the network are provided in Tab.S6 while its performance is assessed in Fig.S3 (for the STW variable) and Fig.S4 (for the CO_2 emission rate).

Regression variable	Hidden layers	alpha	Activation function	Max iterations
STW	112	1.E-04	relu	10,000
CO2rate	155, 25	1.E-05	relu	10,000

Tab.S6 parameters of the multi-layer perceptron of the ferry.

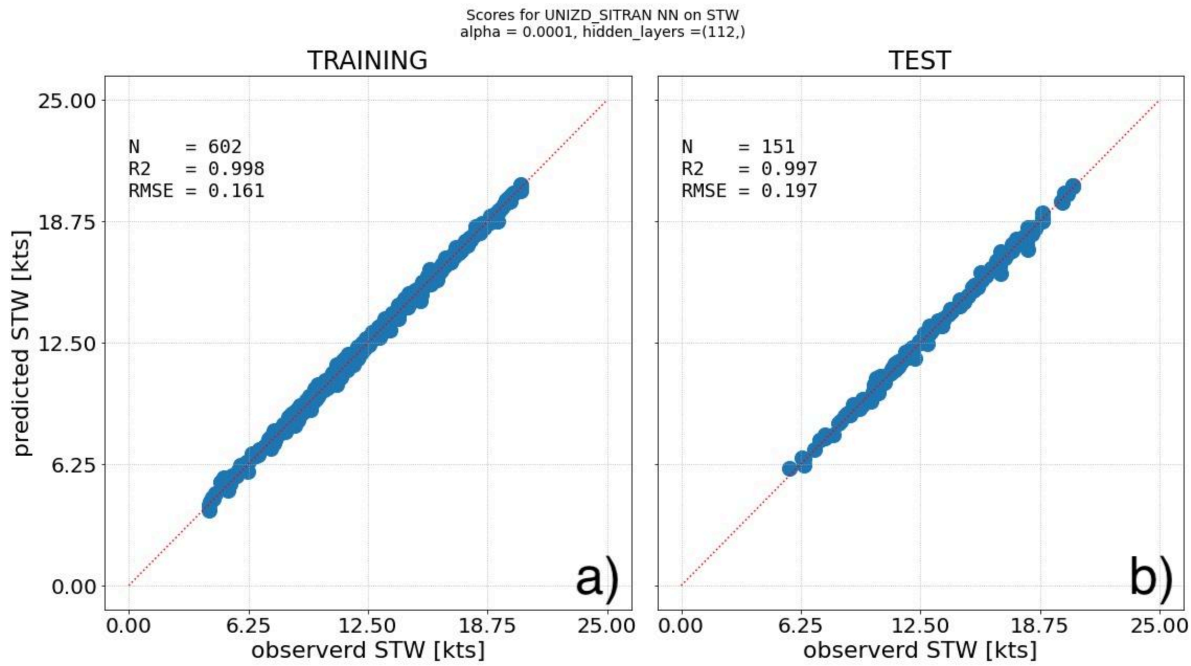

Fig.S3 Predicted vs. observed STW of the ferry for both the training (a) and the test dataset (b) of the neural network, with relative scores printed in the legends.

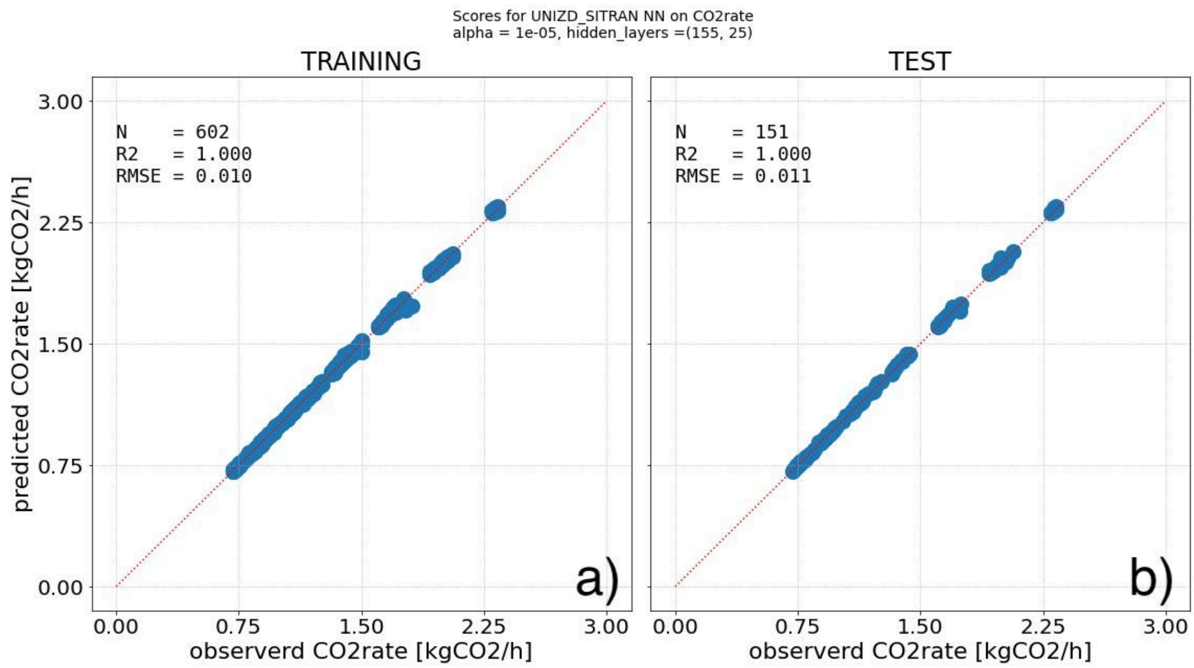

Fig.S4 Predicted vs. observed CO_2 emission rate of the ferry for both the training (a) and the test dataset (b) of the neural network, with relative scores printed in the legends.

S2.2 Sailboat

The sailboat is the about 11-m long Beneteau First-367 vessel which principal particulars are given in Tab.3 of the main manuscript. The scores (Pearson's R^2 coefficient, root mean square error RMSE) from both the spline and neural network are given in the following two subsections. It is distinguished between the speed through water (STW) and the leeway velocity.

S2.2.1 Spline

The Bspline method is used, and the outcome is provided in the figure below.

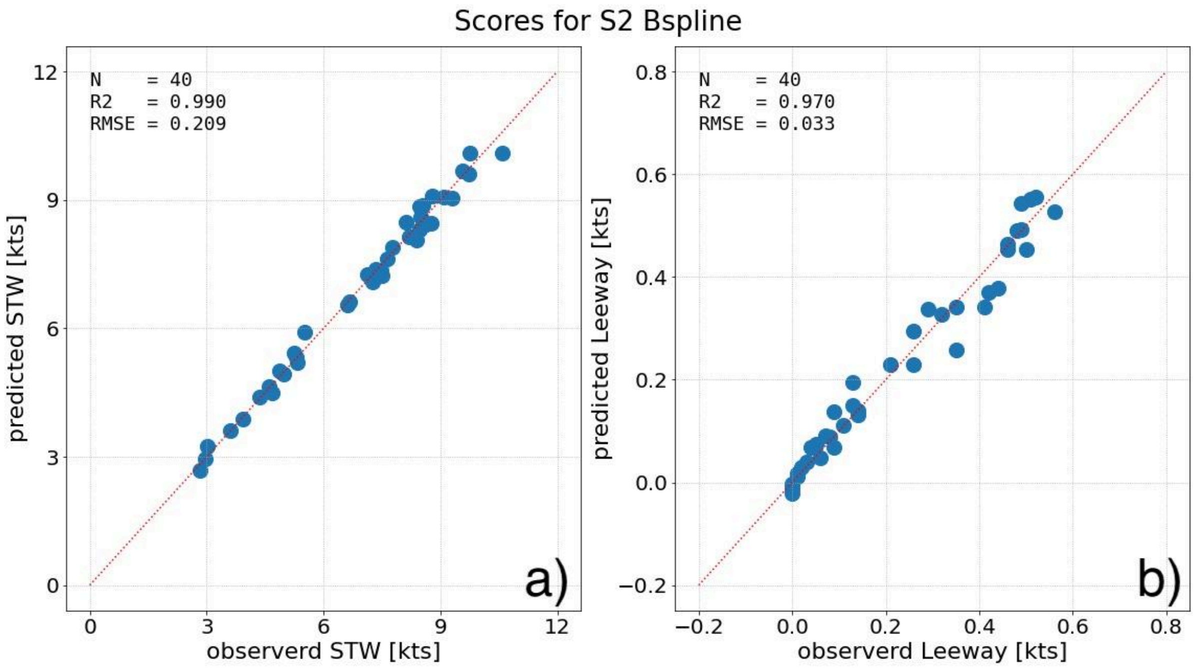

Fig.S5 Predicted vs, observed STW (a) and leeway velocity (b) of the First-367 sailboat, using the spline interpolation on the vessel's LUT.

S2.2.2 Neural Network

The parameters of the network are provided in Tab.S7 while its performance is assessed in Fig.S6 (for the STW variable) and Fig.S7 (for the leeway).

Regression variable	Hidden layers	alpha	Activation function	Max iterations
STW	25, 67	1.E-05	relu	10,000
Leeway	10, 49	1.E-04	relu	10,000

Tab.S7 parameters of the multi-layer perceptron of the sailboat.

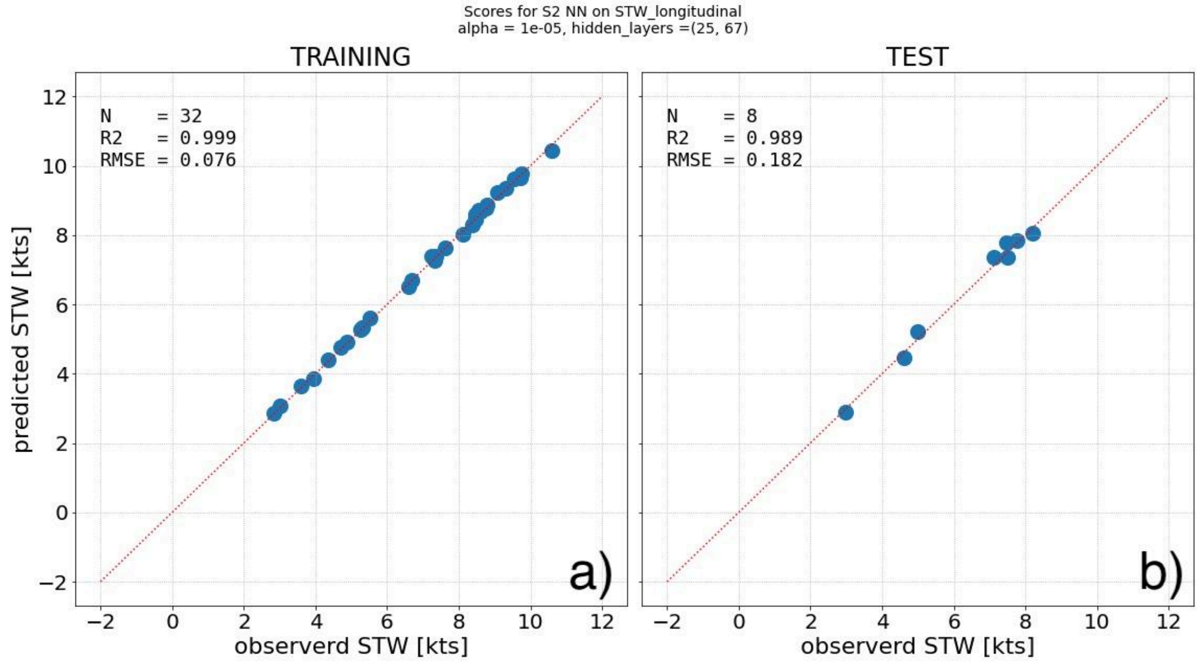

Fig.S6 Predicted vs. observed STW of the sailboat for both the training (a) and the test dataset (b) of the neural network, with relative scores printed in the legends.

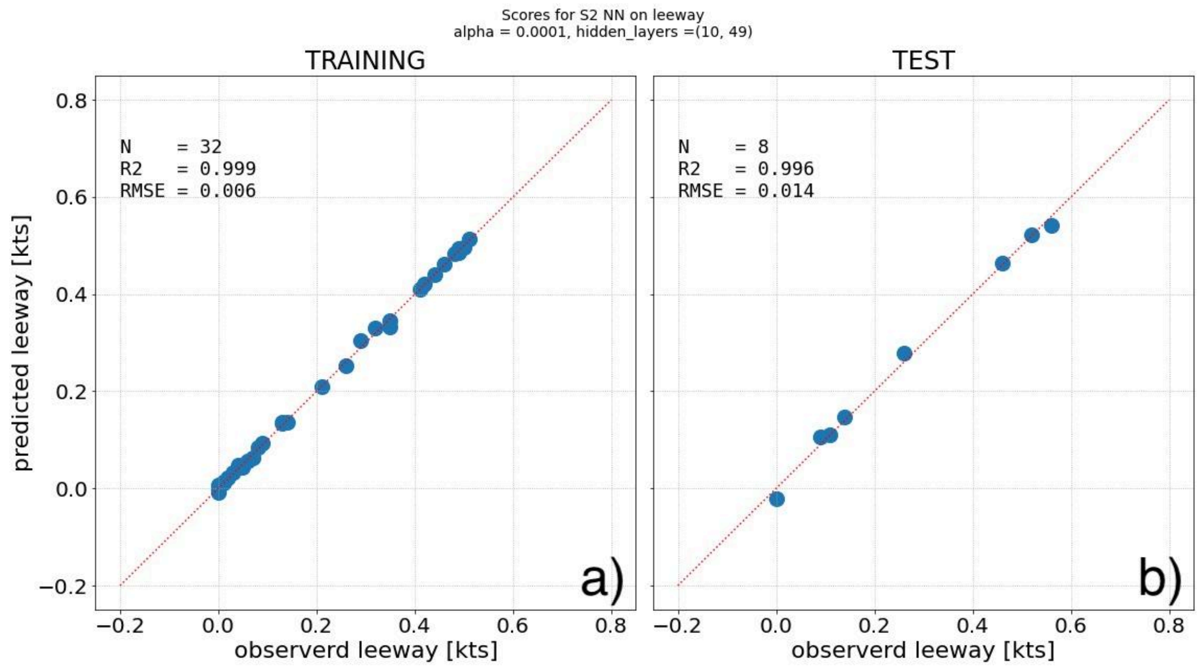

Fig.S7 Predicted vs. observed leeway velocity of the sailboat for both the training (a) and the test dataset (b) of the neural network, with relative scores printed in the legends.

Back to Introduction

S3. Specific routes

In this section, specific and to some extent exceptional routes for both the ferry and the sailboat are presented.

S3.1 Ferry

Among the 2022's numerical experiments, there is just one least-CO2 route sailing East of Sardinia. For this special route it is therefore interesting to evaluate the marine conditions, the CO_2 savings, and the difference with the other optimal routes with the same departure time.

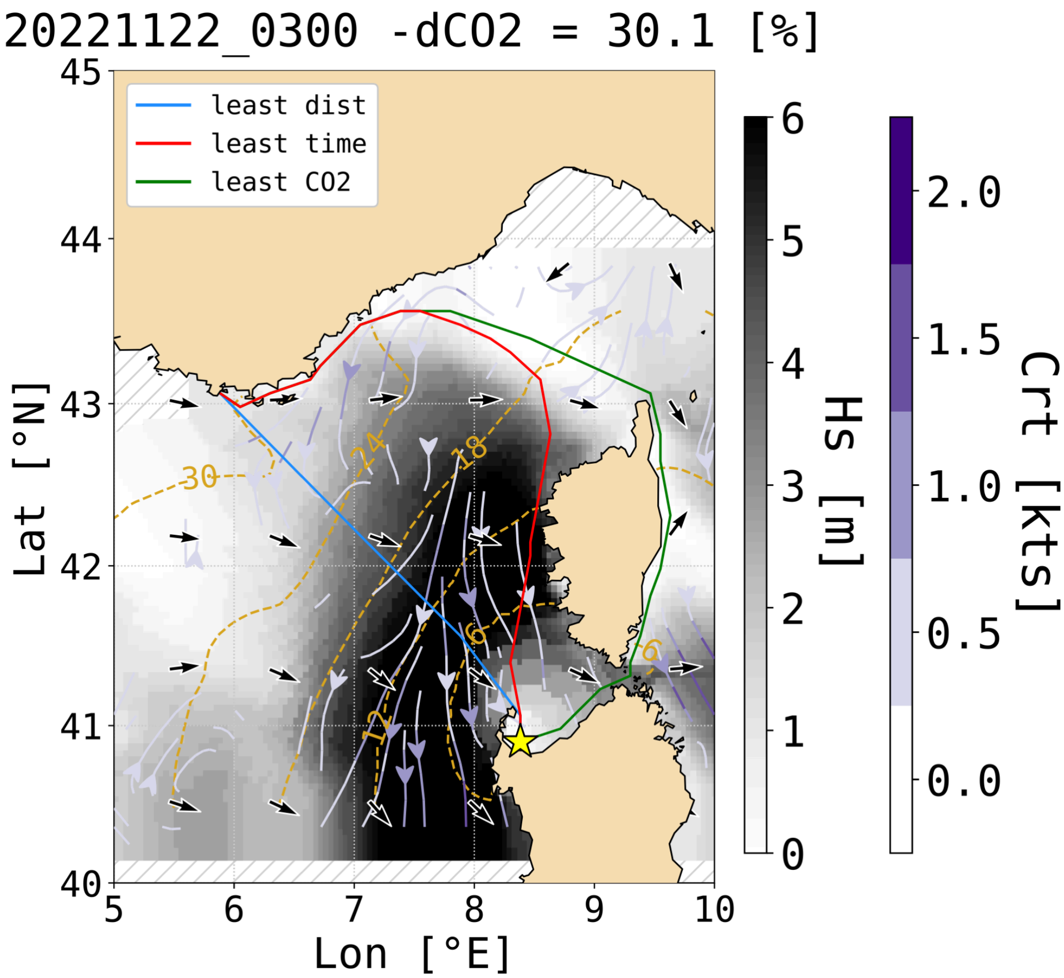

Fig.S8 Optimal Routes of the Ferry. For the specified departure date and time, the least-CO2 route is shown in green, the least-time route in red, and the least-distance route in blue. The significant wave height field is displayed in grey tones with black arrows, while the currents are depicted in purple tones with white streamlines. The algorithm did not utilise environmental field values within the etched area. Additionally, isochrones of the CO_2 -optimal route are shown at 3-hourly intervals. The engine load used was χ = 0.7.

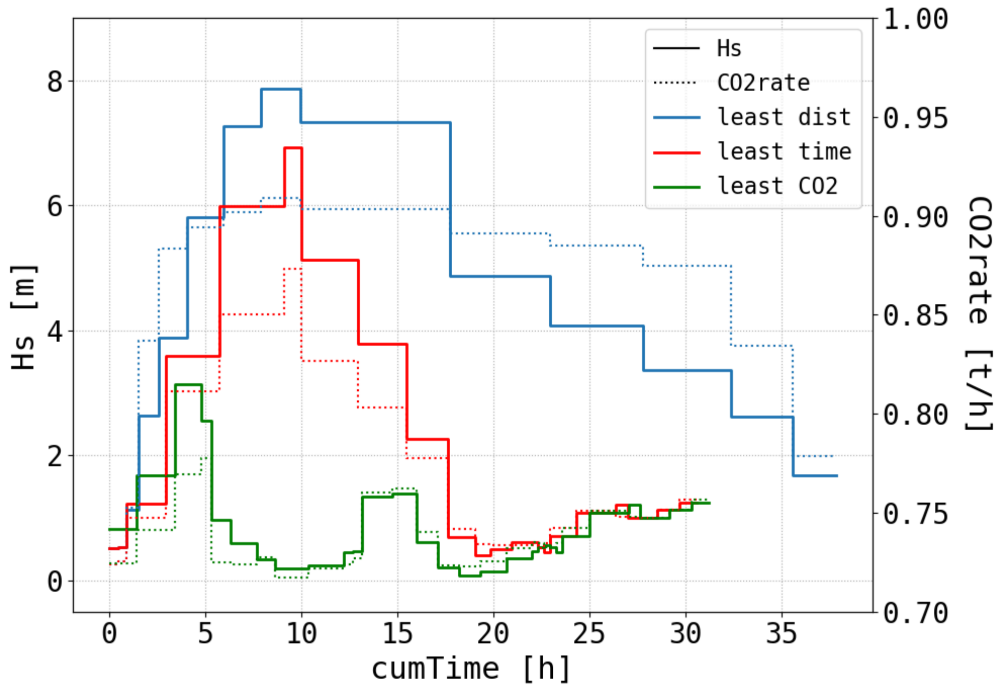

Fig.S9 Time-evolution or linechart of the three optimal routes shown in Fig.S11.

S3.2 Sailboat

Among the numerical experiments conducted in 2022, there are only five instances of least-time sailboat routes with durations longer than their corresponding shortest-distance routes. Relevant data pertaining to these instances is provided in Tab.S8.

	departure	origin	forcing	T* hr	dT* [%]
1	20221007	GRMON	wi-le	32.9078	1.9949
2	20220604	GRMON	wi-le	42.2356	1.2908
3	20220718	GRMON	wi-le	32.2711	0.2572
4	20220721	GRMON	wi	32.1034	0.0101
5	20220209	GRMON	wi	30.7460	1.5280

Tab.S8 non-FIFO least-time routes: departure date and time, origin port, environmental forcing considered (wi: wind; wi-le: both wind and leeway), T*: route duration in hours, dT*: percentage duration increases with respect to corresponding least-distance routes.

To explore the reasons behind why the least-time routes were slower than the least-distance ones, we conducted an analysis focusing on the edges with a termination point at the destination node in Marmaris (for the provided coastal topology and graph connectivity, totaling 11 edges). We considered the corresponding sailing times or edge delays (refer to Eq.17 in the manuscript) at all time steps. Additionally, we found the earliest arrival times at each of these edges (shown as red vertical segments in Fig.S10). The arrival time of the least-distance route was also noted (in blue). Finally, the time for completing the route sailing through these 11 edges was computed.

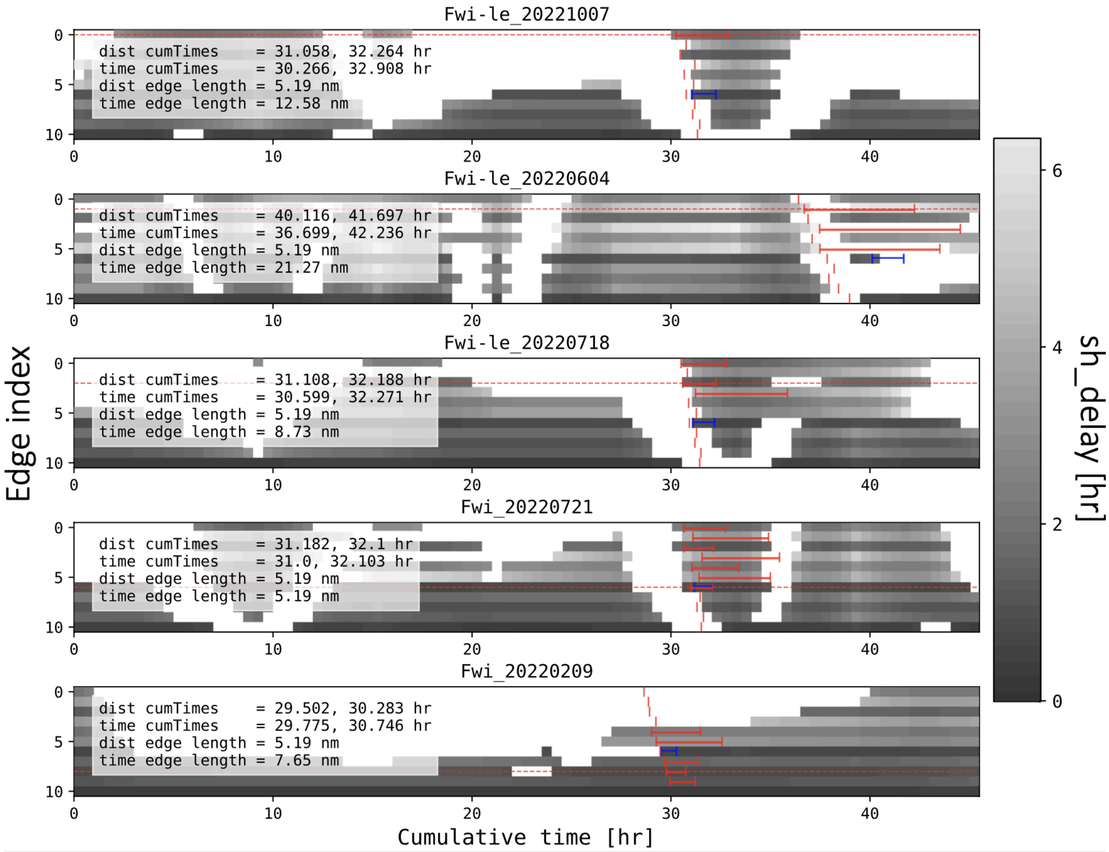

Fig.S10 Heatmap of sailing time for edges ending in the destination node. The five panels refer to the routes in Tab.S8. The red vertical bars on the leftmost side represent the earliest arrival times at each edge. The bars on the rightmost side are corresponding times to reach the destination. The least-time route passes through the edge marked by a horizontal dashed line. Corresponding information for the shortest-distance route is depicted in blue. The arrival times at both the tail and head nodes of the last edge for both types of routes are provided in the legend.

Based on the results depicted in Fig.S10, the three routes accounting for leeway (departures on Oct. 7th, June 4th, and July 18th) reveal that, although the least-time solution accesses its final edge sooner than the least-distance route, it faces adverse sailing conditions (indicated by a lighter shade of grey in the heatmap) compared to those encountered by the least-distance route. In such scenarios, the sailboat following the least-time route will sail at a slower speed compared to an identical vessel on the least-distance route, potentially leading to a delayed arrival at the destination. When this occurs, as for the first three routes, the situation is referred to as non-FIFO (First In, First Out): reaching an intermediate waypoint first does not ensure being the first to arrive at the destination.

For the route departing on Jul. 21st, the durations of both least-distance and least-time route are similar within a margin of 10^{-3} hours, and both routes traverse the same final edge. However, the least-time route accesses the edge earlier than the least-distance one, encountering less favourable wind conditions and consequently arriving at the destination slightly later than the least-distance route.

For the route beginning on Feb. 9th, the least-time route would indeed arrive at the final edge (#7) slightly earlier than the least-distance route, but it would encounter unfavourable sailing conditions, resulting in zero speed over ground. If it could pause and wait for improved environmental conditions, it could eventually align with the shortest distance route, reaching the destination at precisely the same time. As this is not accounted for in the current algorithm, it selects a path through another edge (#9), resulting in a delayed arrival compared to the shortest distance route.

Further advancements in the least-time algorithm of VISIR-2, aligned with the methodology suggested by Orda and Rom (1990), are necessary to address the non-FIFO characteristics of these routes.

Back to Introduction

S4. Bundles

Here the bundles comprising the solutions for all departure dates in 2022, both orientations, and several combinations of dynamic environmental fields are provided.

S4.1 Ferry

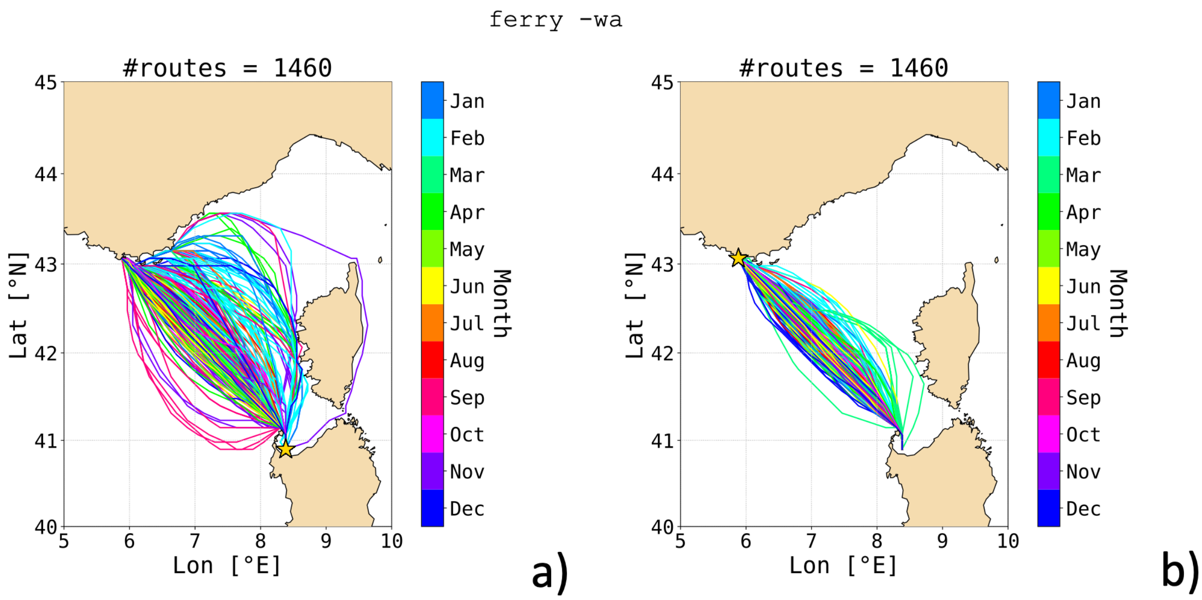

Fig.S11 Bundles for the ferry in case of a) northbound and b) southbound routes. Solutions for all the four engine load values χ = [70,80,90,100]% are shown. Just waves were accounted for.

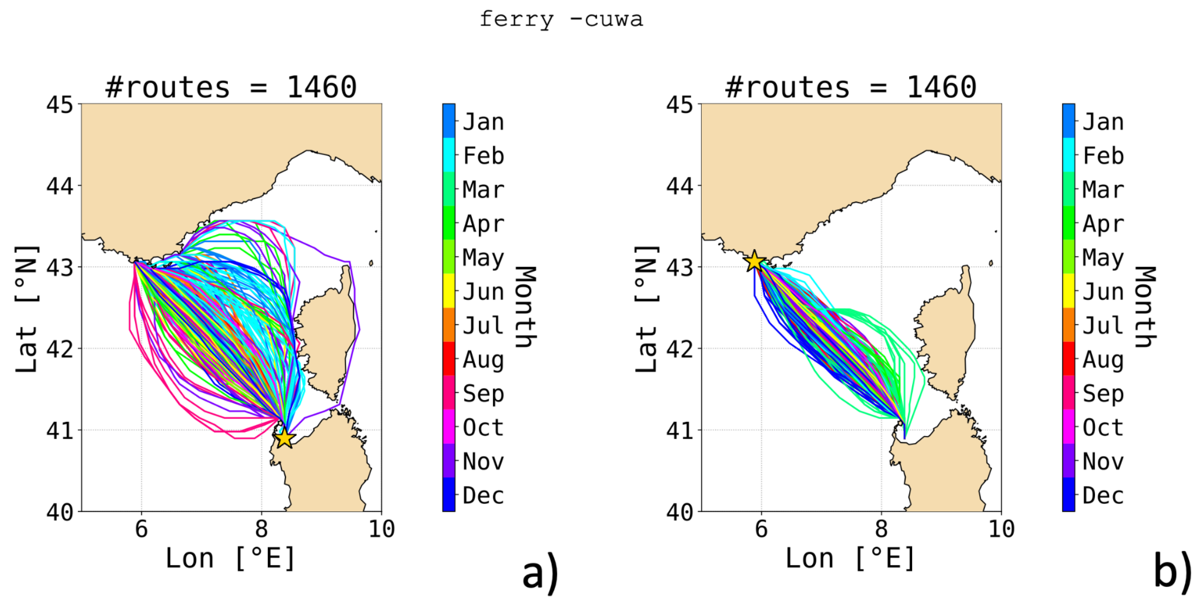

Fig.S12 As S11, but accounting for both waves and currents. Panel a) is identical to Fig.10b of the main manuscript.

S4.2 Sailboat

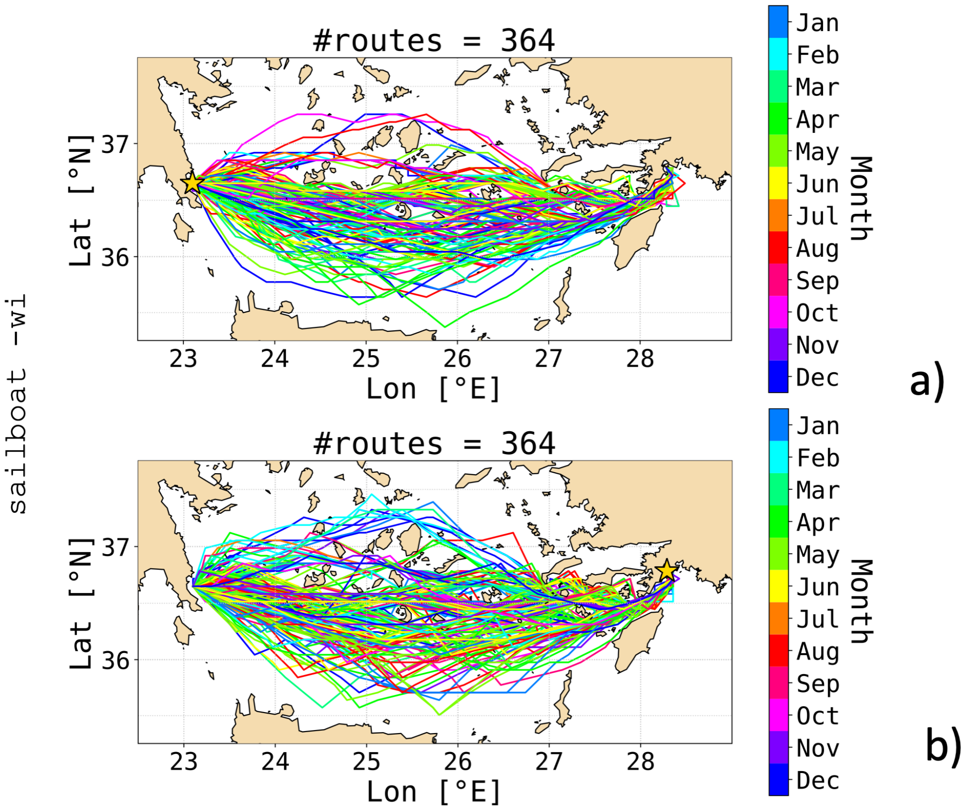

Fig.S13 Bundles for the First-367 sailboat in case of a) eastbound and b) westbound routes. Just wind was accounted for.

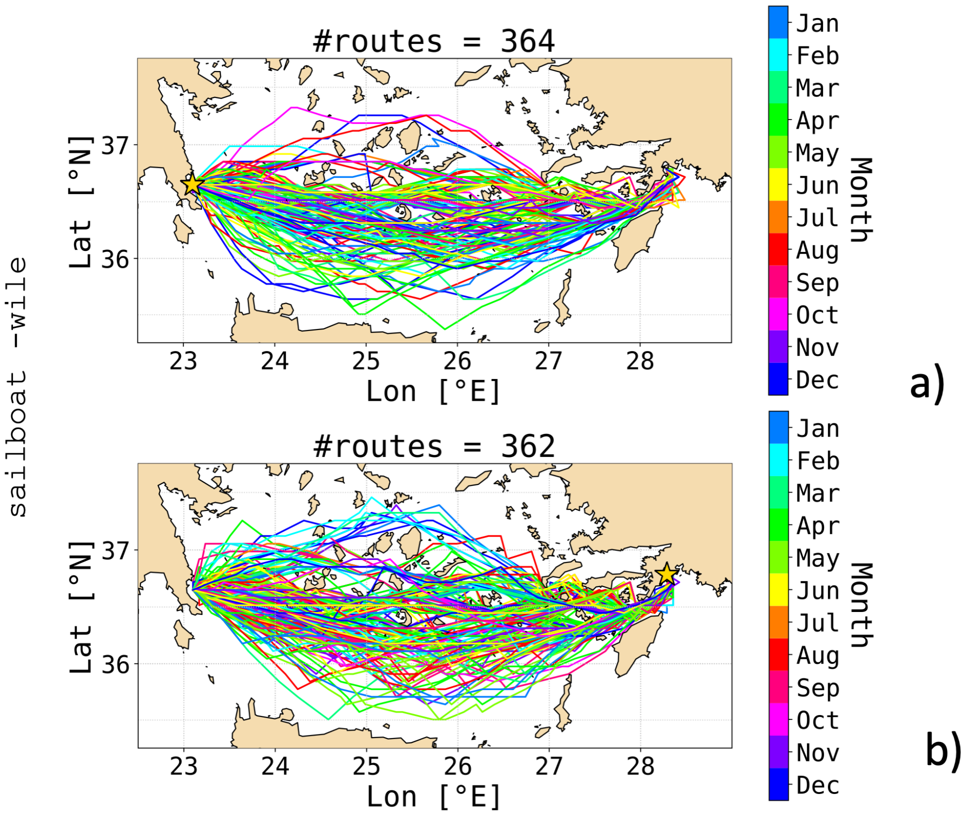

Fig.S14 As Fig.S13, but accounting for both wind and leeway.

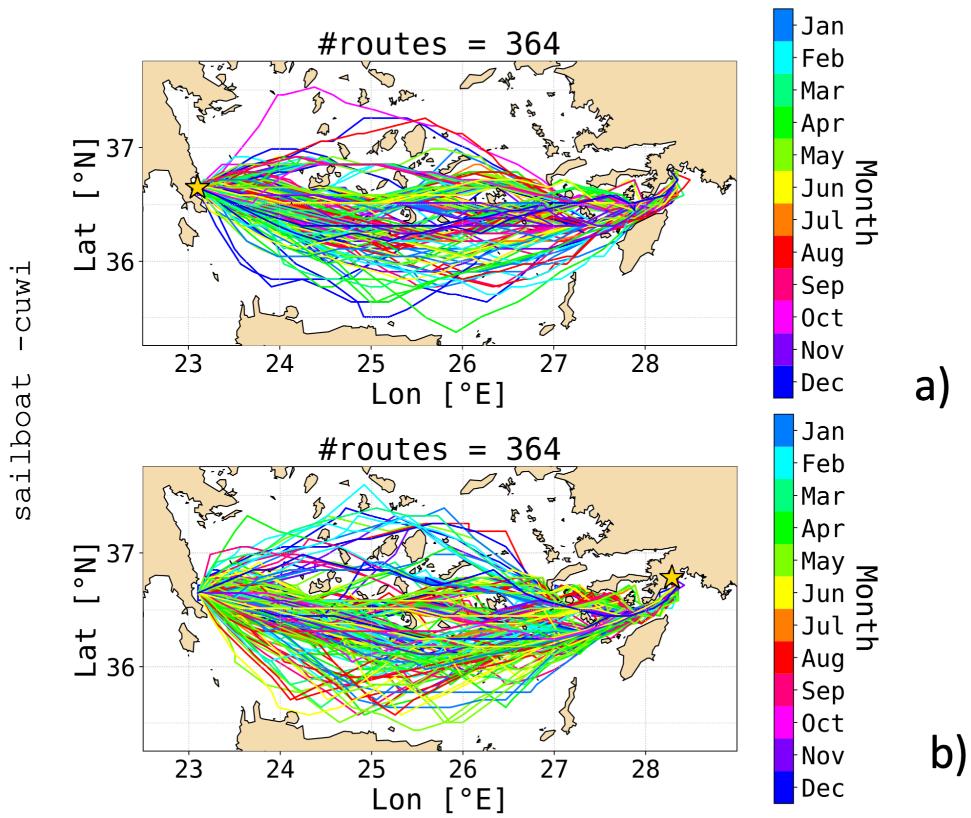

Fig.S15 As Fig.S13, but accounting for both wind and currents. Panel a) is identical to Fig.13b of the main manuscript.

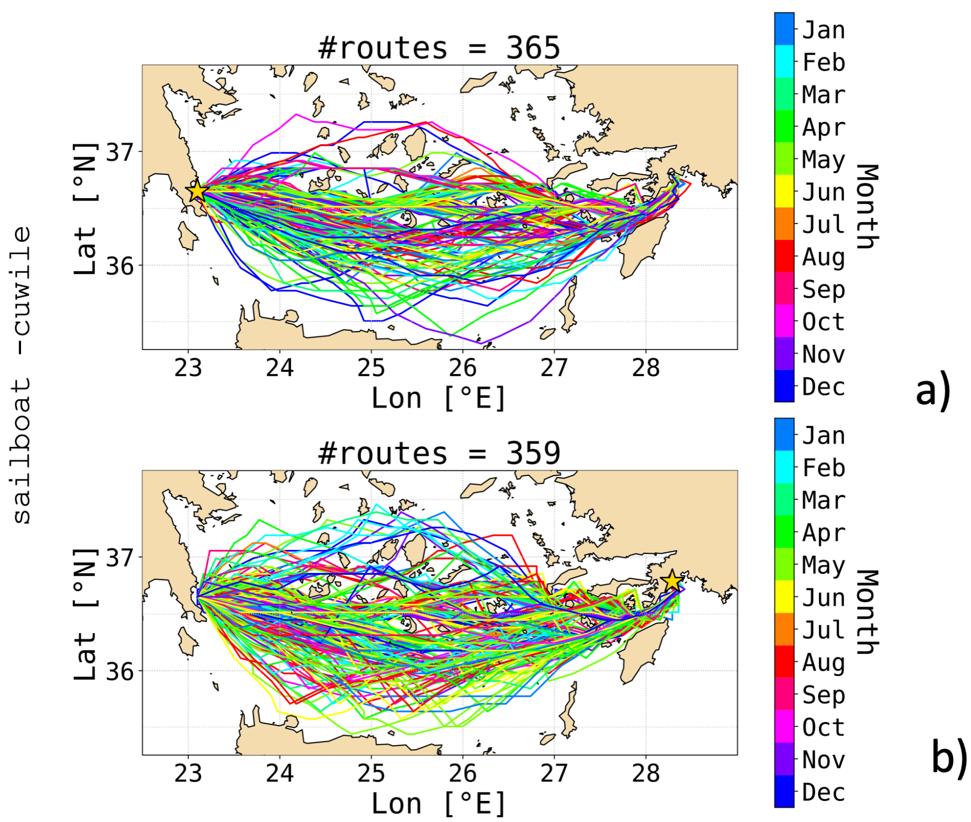

Fig.S16 As Fig.S13, but accounting for wind, leeway, and currents.
Back to Introduction

S5. Sailboat route metrics

Here the duration savings of the sailboat routes shown in Fig. 13 of the manuscript are broken out, depending on the sailing direction.

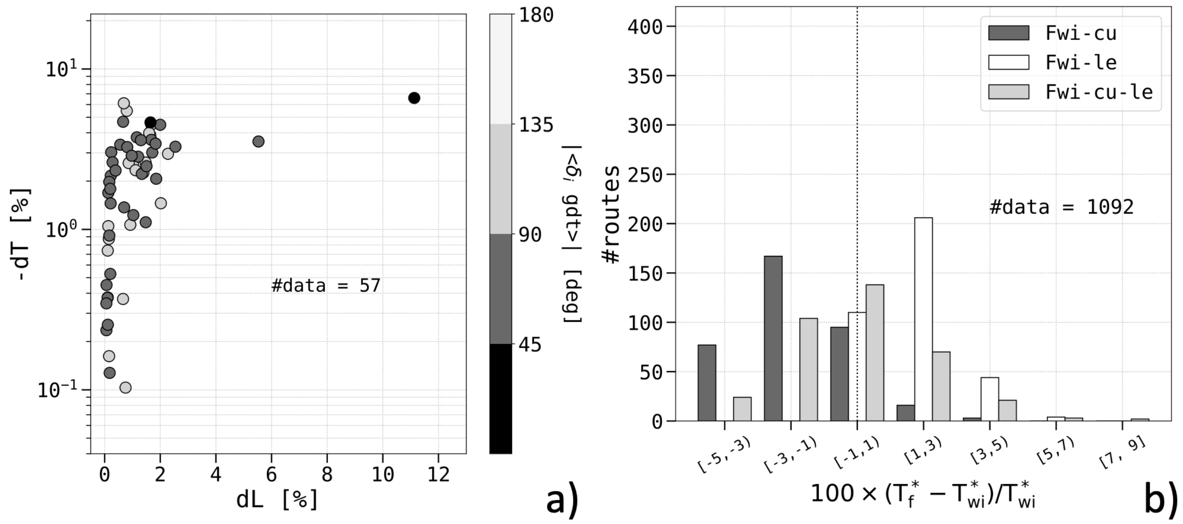

Fig. S17 For westbound routes (TRMRM-GRMON) only: a) Scatter plot of duration relative savings *-dT** vs. relative lengthening *dL* of optimal routes. The marker shape represents the average angle of attack of wind $|<\delta_i^{(gdt)}>|$ along the least-distance route as in legend. b) Histograms of relative route duration T^*_f with forcing combination *f* defined by the column colour, with respect to the duration T_{wi} of the wind-only optimal routes.

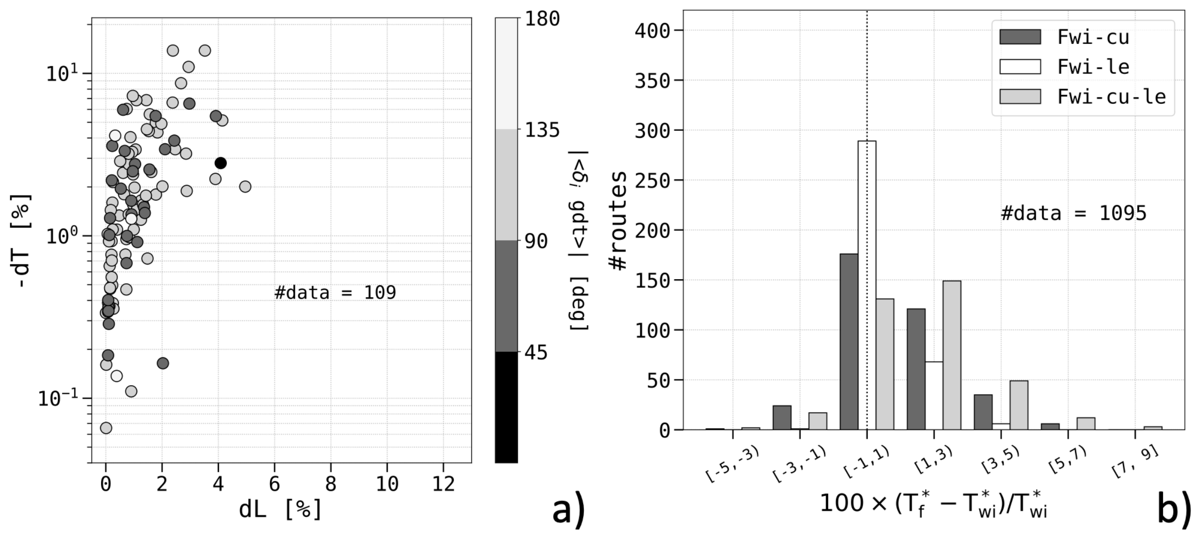

Fig. S18 as Fig.S17 but for eastbound routes (GRMON-TRMRM).

Departure	Forcing	Type	count	mean	std	min	25p	50p	75p	max
GRMON	Fwi	dist	109	0.0	0.0	0.0	0.0	0.0	0.0	0.0
GRMON	Fwi	time	109	-2.49	2.62	-13.82	-3.33	-1.64	-0.77	1.53
GRMON	Fwi-le	dist	89	0.0	0.0	0.0	0.0	0.0	0.0	0.0
GRMON	Fwi-le	time	89	-2.32	2.48	-13.78	-2.94	-1.52	-0.75	1.99
GRMON	Fcu-wi	dist	111	0.0	0.0	0.0	0.0	0.0	0.0	0.0
GRMON	Fcu-wi	time	111	-3.12	2.84	-14.58	-4.09	-2.4	-1.19	-0.21
GRMON	Fcu-wi-le	dist	98	0.0	0.0	0.0	0.0	0.0	0.0	0.0
GRMON	Fcu-wi-le	time	98	-3.21	2.72	-13.7	-4.14	-2.48	-1.34	-0.19
TRMRM	Fwi	dist	57	0.0	0.0	0.0	0.0	0.0	0.0	0.0
TRMRM	Fwi	time	57	-2.34	1.59	-6.6	-3.37	-2.33	-1.05	-0.1
TRMRM	Fwi-le	dist	37	0.0	0.0	0.0	0.0	0.0	0.0	0.0
TRMRM	Fwi-le	time	37	-2.42	1.71	-6.26	-3.38	-2.47	-0.85	-0.1
TRMRM	Fcu-wi	dist	45	0.0	0.0	0.0	0.0	0.0	0.0	0.0
TRMRM	Fcu-wi	time	45	-3.06	1.78	-7.44	-3.97	-3.05	-1.52	-0.32
TRMRM	Fcu-wi-le	dist	39	0.0	0.0	0.0	0.0	0.0	0.0	0.0
TRMRM	Fcu-wi-le	time	39	-3.53	2.07	-8.8	-4.59	-3.56	-1.83	-0.34

Tab. S9 Statistics of sailboat route duration percentage savings for various route origin (GRMON or TRMRM), forcings (wind: wi, currents: cu; leeway: le), optimisation objectives (least-distance or least-time). The number of routes (count), their mean duration (mean) and standard deviation in hours (std), their minimum and maximum (min, max) value, 25th, 50th, 75th percentiles are provided.

[Back to Introduction]

S6. Angle of attack

Here various plots regarding the computation of the angle attack δ between vessel's heading and course are provided.

S6.1 Ferry

The results in this section refer to the ferry described in the main manuscript.

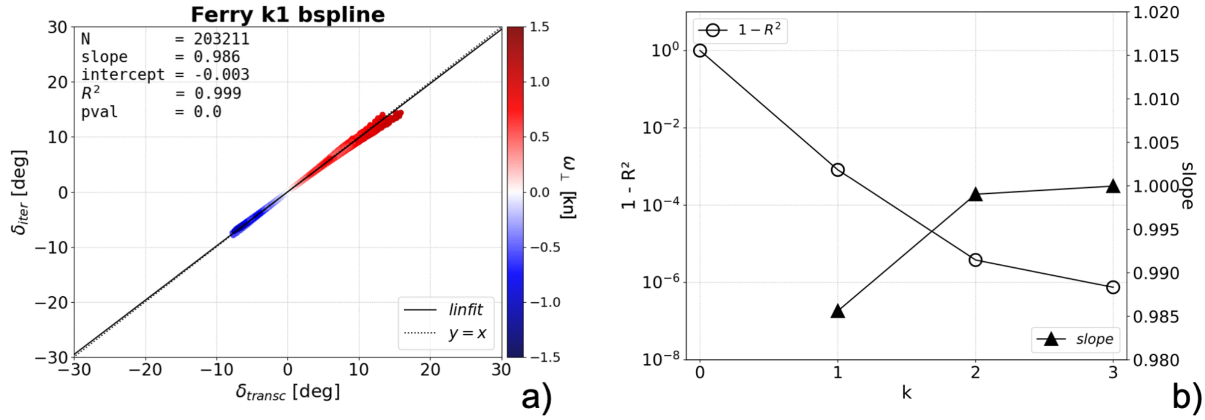

Fig. S19 Approximate vs. exact solution of Eq. 13 of the main manuscript, for the ferry. a) Iterative solution of Eq. A1 with *k* = 1 vs. exact solution, using the cross component of the effective flow $\omega_\perp$ as marker colour; b) unexplained variance (*R* is the Pearson's correlation coefficient) of the linear regression and fitted slope coefficient for various *k* values. The vessel's LUT was fitted via the neural network as explained in the main manuscript.

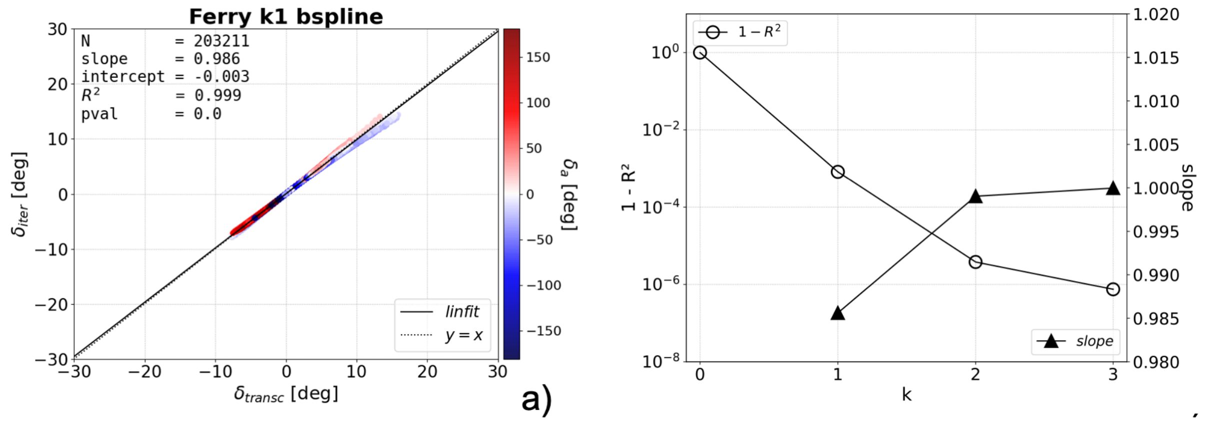

Fig. S20 As Fig.S17 but with wave angle of attack δ_a as marker colour.

S6.2 Sailboat

The results in this section refer to the sailboat described in the main manuscript (Sect. 4.2.1) and to some additional vessels (Sect. 4.2.2).

S6.2.1 First-367

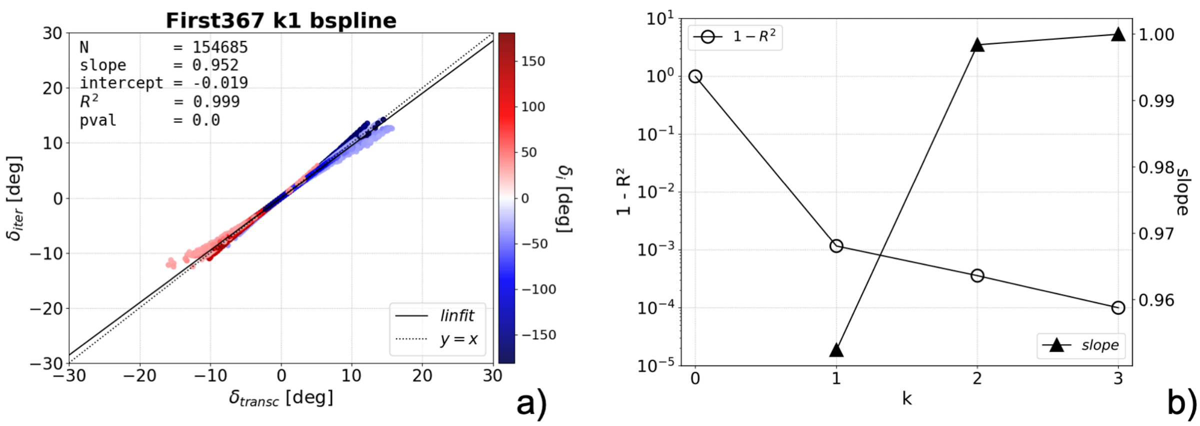

Fig. S21 Approximate vs. exact solution of Eq. 13 of the main manuscript, for the sailboat. a) Iterative solution of Eq. A1 with *k* = 1 vs. exact solution, using the cross component of the wind angle of attack δ_i as marker colour; b) unexplained variance (*R* is the Pearson's correlation coefficient) of the linear regression and fitted slope coefficient for various *k* values. The vessel's LUT was fitted via a cubic spline.

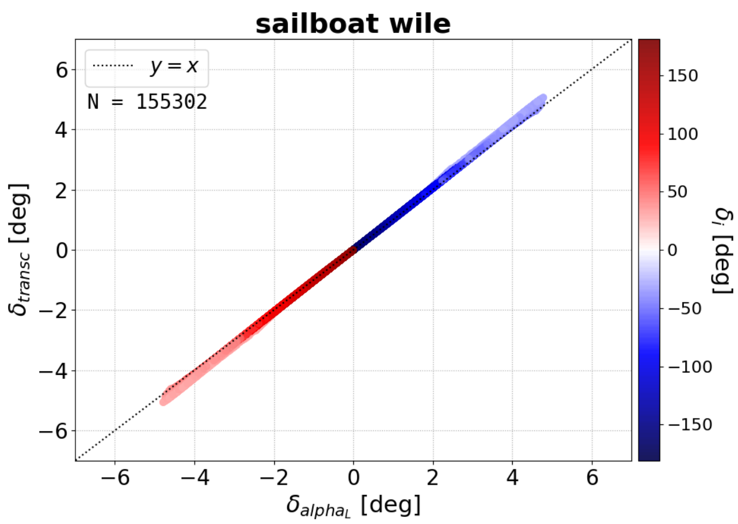

Fig. S22 Angle of attack δ from the exact solution of manuscript's Eq. 13 vs. the analytic solution in the absence of currents (Eq. 6). The marker colour refers to the wind angle of attack δ_i.

S6.2.2 Other sailboats

J24

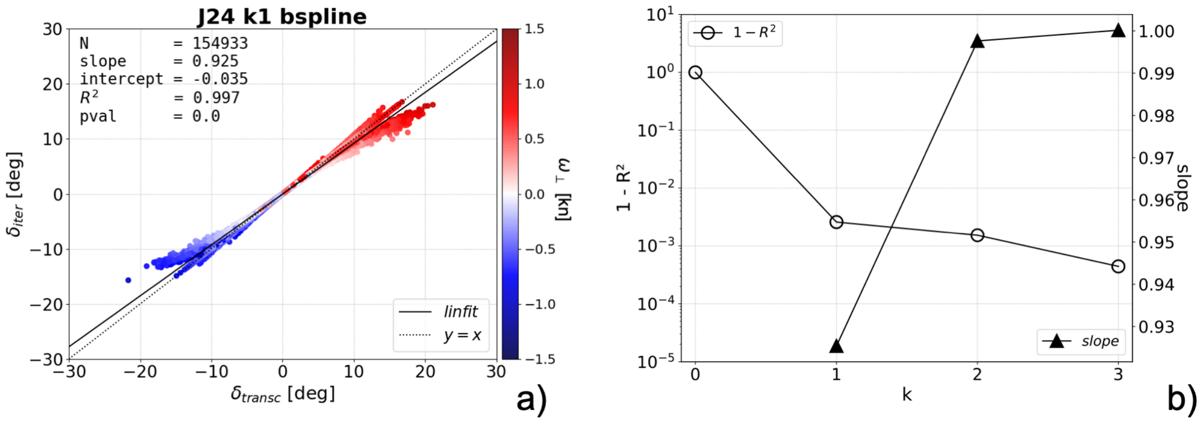

Fig. 23 Approximate vs. exact solution of Eq. 13 for a J24 sailboat. a) Iterative solution of Eq. A1 with *k* = 1 vs. exact solution, using the cross component of the effective flow $\omega_\perp$ as marker colour; b) unexplained variance (*R* is the Pearson's correlation coefficient) of the linear regression and fitted slope coefficient for various *k* values.

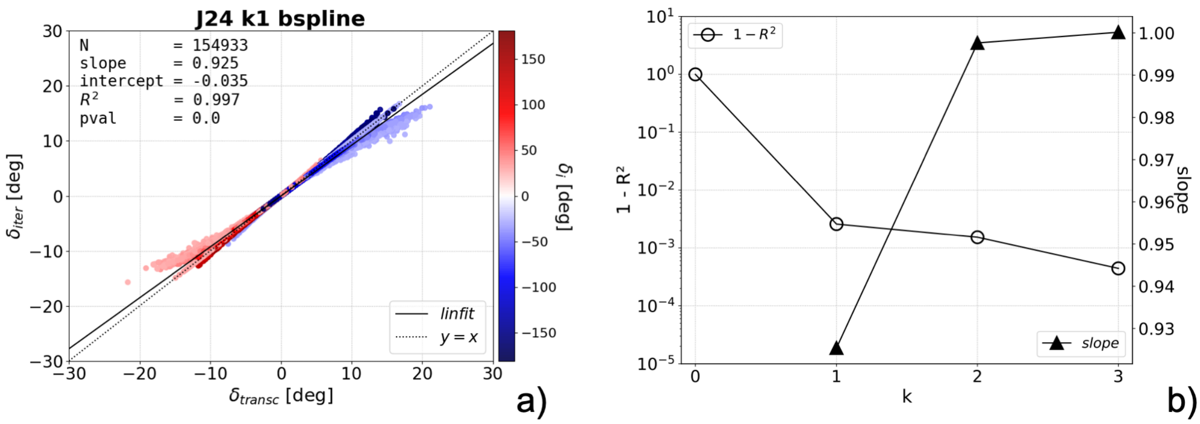

Fig. S24 As Fig.S23, but using the relative wind angle δ_i as marker colour.

Swan60FD

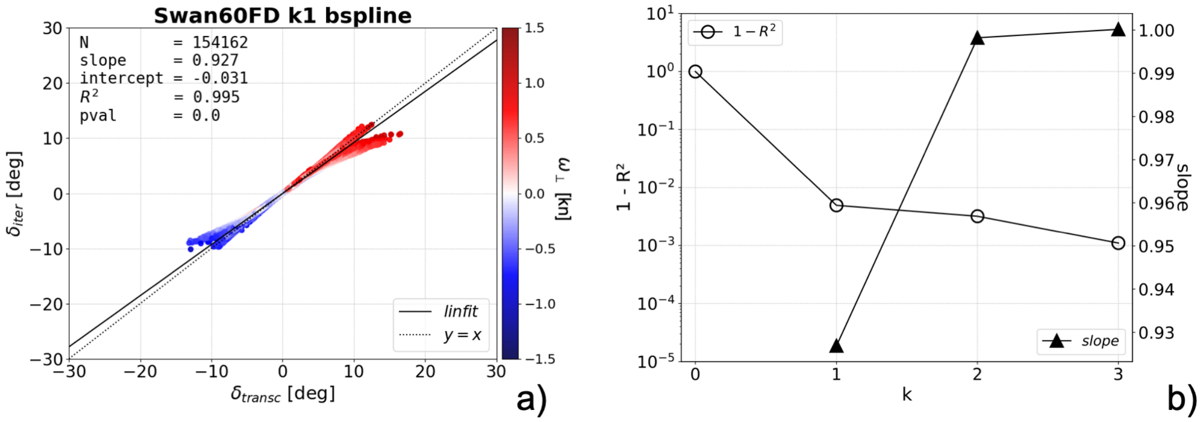

Fig. S25 Approximate vs. exact solution of Eq. 13 for a Swan-60FD sailboat. a) Iterative solution of Eq. A1 with *k* = 1 vs. exact solution, using the cross component of the effective flow $\omega_\perp$ as marker colour; b) unexplained variance (*R* is the Pearson's correlation coefficient) of the linear regression and fitted slope coefficient for various *k* values.

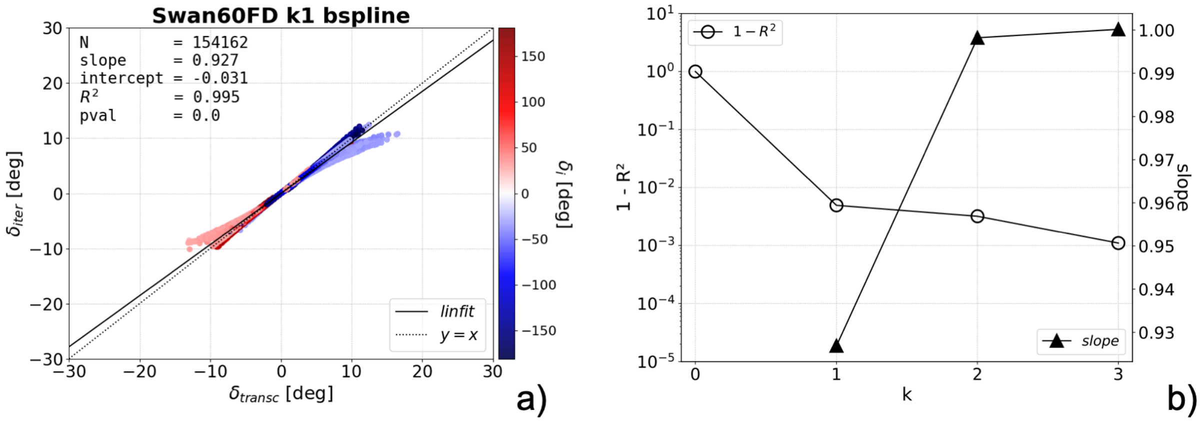

Fig. S26 As Fig.S25, but using the relative wind angle δ_i as marker colour.

Back to Introduction